Journal of Glaciology

Paper

Cite this article: Cerrato R, Salvatore MC, Gunnarson BE, Linderholm HW, Carturan L, Brunetti M, Baroni C (2020). *Pinus cembra* L. tree-ring data as a proxy for summer mass-balance variability of the Careser Glacier (Italian Rhaetian Alps). *Journal of Glaciology* 1–13. https://doi.org/10.1017/jog.2020.40

Received: 26 April 2019
Revised: 5 May 2020
Accepted: 6 May 2020

Keywords:
Climate change; glacier fluctuations; glacier mass balance; mass-balance reconstruction

Author for correspondence:
Carlo Baroni, E-mail: carlo.baroni@unipi.it

Pinus cembra L. tree-ring data as a proxy for summer mass-balance variability of the Careser Glacier (Italian Rhaetian Alps)

Riccardo Cerrato[1], Maria Cristina Salvatore[1,2], Björn E. Gunnarson[3], Hans W. Linderholm[4], Luca Carturan[5], Michele Brunetti[6] and Carlo Baroni[1,2]

[1]Dipartimento di Scienze della Terra, University of Pisa, Pisa, Italy; [2]CNR–IGG, Consiglio Nazionale delle Ricerche–Istituto di Geoscienze e Georisorse, Pisa, Italy; [3]Department of Physical Geography, Stockholm University, Stockholm, Sweden; [4]Department of Earth Sciences, University of Gothenburg, Gothenburg, Sweden; [5]Dipartimento Territorio e Sistemi Agro–Forestali, University of Padova, Italy and [6]CNR–ISAC, Consiglio Nazionale delle Ricerche–Istituto di Scienze dell'Atmosfera e del Clima, Bologna, Italy

Abstract

Glacial extent and mass balance are sensitive climate proxies providing solid information on past climatic conditions. However, series of annual mass-balance measurements of more than 60 years are scarce. To our knowledge, this is the first time the latewood density data (MXD) of the Swiss stone pine (*Pinus cembra* L.) have been used to reconstruct the summer mass balance (B_s) of an Alpine glacier. The MXD-based B_s well correlates with a B_s reconstruction based on the May to September temperature. Winter precipitation has been used as an independent proxy to infer the winter mass balance and to obtain an annual mass-balance (B_n) estimate dating back to the glaciological year 1811/12. The reconstructed MXD/precipitation-based B_n well correlates with the data both of the Careser and of other Alpine glaciers measured by the glaciological method. A number of critical issues should be considered in both proxies, including non-linear response of glacial mass balance to temperature, bedrock topography, ice thinning and fragmentation, MXD acquisition and standardization methods, and finally the 'divergence problem' responsible for the recently reduced sensitivity of the dendrochronological data. Nevertheless, our results highlight the possibility of performing MXD-based dendroglaciological reconstructions using this stable and reliable proxy.

1. Introduction

Global warming over the last decades has been well documented (IPCC, 2013, 2018), and its effects are particularly evident in mountainous regions (Beniston and others, 1997; Pepin and others, 2015), and especially in the European Alps, where temperatures are increasing more than the global average (Böhm and others, 2001; Auer and others, 2007; Brunetti and others, 2009). This makes Alpine regions vulnerable to changes in the hydrological cycle and to decreases in snow and glacier cover (WGMS and NSIDC, 2012; IPCC, 2019). The recent increase in temperatures has turned mountainous areas into progressive deglaciations, since glaciers have a sensitive response to climate variations through changes in volume and geometry (Oerlemans, 2001; Zemp and others, 2015; Huss and others, 2017). Solid information on past climatic conditions can be provided by recognized sensitive indirect (e.g. glacial extent and glacier length) and direct (e.g. mass balance) climate proxies (Lowe and others, 2008; Ivy-Ochs and others, 2009; Baroni and others, 2017b). However, very few long-term and annually resolved series of measurements of past glacial mass-balance variations extending beyond the past few decades exist but, since the annual mass balances of glaciers are mainly influenced by climatic factors (Oerlemans, 2001; Zemp and others, 2015), other proxies sensitive to the same factors may be used for the reconstruction of past mass-balance series. For instance, the variability of summer and annual balance is closely related to temperatures during the ablation period (Zemp and others, 2015; Carturan and others, 2016; Huss and others, 2017). Thus, proxies sensitive to mean temperatures of the ablation season can be used to extend glacier summer balance records back in time in areas like the Italian Alps, where the latter parameter is mainly influenced by temperature (Carturan and others, 2016).

Several studies have successfully used tree-ring proxies to reconstruct past temperature variabilities (Büntgen and others, 2005; Wilson and others, 2016; Anchukaitis and others, 2017; Esper and others, 2018), as well as glacial mass-balance fluctuations in North America, Fennoscandia and the European Alps (Nicolussi, 1995; Watson and Luckman, 2004; Larocque and Smith, 2005; Linderholm and others, 2007; Leonelli and others, 2011; Wood and Smith, 2013, 2015). For instance, Watson and Luckman (2004) used a tree-ring width (TRW) chronology from mixed conifers (*Larix lyallii* Parl., *Picea engelmannii* Parry ex Engelm. and *Pinus albicaulis* Engelm.) to build a model explaining ~40% of the observed summer mass balance of the Peyto Glacier (Canada). Similarly, Linderholm and others (2007) used tree-ring density (MXD) and TRW from the Scots pine (*Pinus sylvestris* L.) to reconstruct the

summer mass balance of Storglaciären in Sweden and they succeeded in explaining ~50% of the observed variance. Studies in the European Alps have attempted to reconstruct annual glacier mass balances. In the Ötztaler Alps (Austria), Swiss stone pine (*Pinus cembra* L.) tree-ring chronologies were used to infer variations in the Hintereisferner (Nicolussi, 1995), but in the Rhaetian Alps (Italy), no stable association could be found between TRWs from the same species and climate nor annual glacial mass balances (Leonelli and others, 2011).

The selection of proxies for reconstructing past glacial variations is fundamental. Several tree-ring parameters can be used to infer past climatic variations, such as TRW, MXD, blue intensity and stable isotopes (Schweingruber, 1988; Robertson and others, 2008; Björklund and others, 2019). MXD usually gives higher correlations with mean summer temperatures since this parameter is less prone than TRW to non-climatic interferences (Briffa and others, 2004; Kirdyanov and others, 2006; Büntgen and others, 2011; Konter and others, 2016; Ljungqvist and others, 2020). A higher correlation between MXD and temperature compared to TRW was demonstrated for the European larch (*Larix decidua* Mill.) (Büntgen and others, 2006) and the Scots pine from different regions (Gunnarson and others, 2011; Linderholm and others, 2015). However, the density analysis of the Swiss stone pine, which, in addition to the larch, characterizes the treeline in Alpine ranges, has been widely overlooked. In fact, only the width of the tree-rings (i.e. total ring, earlywood and latewood widths) has been used when assessing the association of this species with temperatures and glacial frontal variations (Nicolussi, 1995; Oberhuber, 2004; Carrer and Urbinati, 2006; Leonelli and others, 2008).

The aim of this paper is to explore the possibility of reconstructing the summer mass balance of the Careser Glacier in the Rhaetian Alps using the Swiss stone pine MXD, which has recently shown to be sensitive to mean temperature during the whole ablation season (May–September; Cerrato and others, 2019). The measured annual mass balance of the Careser Glacier was selected as predictand due to the length of this time series, which (i) permits a higher degree of freedom during calibration of the models; and (ii) covers the last glacier advance recorded in the Alps during the 1970s and 1980s. The MXD-based reconstructions were also compared to an independent reconstruction obtained by means of instrumental temperatures. Additionally, the instrumentally measured winter precipitation was used as an independent predictor to infer the winter mass balance and to reconstruct the full annual mass-balance record back to 1811/12.

2. Study area

This study focuses on the Careser Glacier, which is located in the Ortles-Cevedale Group of the southern Italian Rhaetian Alps (Fig. 1). The Alpine Arch is described as a transitional region characterized by at least three climatic zones (Atlantic in the West, Mediterranean in the South and European continental in the North), and the topographic effects have a relevant influence over these zones (Auer and others, 2007). Along the chain, a strong latitudinal pattern is noticeable where the wetter zones are distributed along the southern and northern rims (Isotta and others, 2014). The elevation highly contributes to this precipitation pattern by sheltering the inner portion of the mountain range from the moisture-carrying winds, thus inducing the so-called 'inner dry Alpine zone'.

On the southern margin of the Alps, the climate regime changes significantly over a relatively short distance. In fact, from a climate described as temperate, according to the Köppen–Geiger classification (Peel and others, 2007), which is without a dry season but with hot summers (Cfa) observed in the Po plain, the climate conditions become typical of a Polar tundra (ET) at the highest peaks. The Ortles-Cevedale Group is located southward to the 'inner dry Alpine zone' (Isotta and others, 2014). The recorded precipitation quantity increases to the south and with elevation. A total annual precipitation of 1300–1500 mm has been estimated at 3000–3200 m a.s.l. in the area of the Careser Glacier (Carturan and others, 2012), whereas the meteorological station of the Careser dam (2606 m a.s.l.) reports a mean annual precipitation of 1200 mm during the 1961–90 period (Fig. S1 in Supplementary Material).

The Careser Glacier (46.45202°N, 10.71700°E) is a mountain glacier located in the south-eastern portion of the Ortles-Cevedale Group (southern Rhaetian Italian Alps), which is the largest glaciated mountain group of the Italian Alps (Carturan and others, 2013b; Salvatore and others, 2015). The glacier represents a unique case in the Italian Alps, owing to its long-term measured mass-balance continuous series of more than 40 years, and to the front variation fragmented series starting in 1897. Nowadays, the glacier is nested in a wide, south-facing cirque surrounded by metamorphic rock peaks (micaschists and phyllites). The glacier presents a rather flat surface, covering an area of 1.63 km^2 in 2012. Recently, this glacier has been divided into three main ice bodies and three smaller ice patches caused by accelerated decay, but this effect is only the last expression of a long-term retreatment that started at the end of the 19th century (Carturan and others, 2013a). The glacier's winter mass balance is mainly associated with precipitation and wind-drifted snow, whereas avalanches and topographic shading are of minor importance. In contrast, the summer mass balance is mainly driven by mean temperatures of the May to September period (Carturan and others, 2013a; Baroni and others, 2018).

3. Materials and methods

3.1 Tree-ring data

Tree-ring sampling of Swiss stone pine was performed at the treeline between 2075 and 2350 m a.s.l. in the Upper Peio Valley, which is close to the Careser Glacier (46°25.2′N, 10°41.1′E, Fig. 1). The sampling area is close to the boundary of the natural distribution range of the species (http://www.euforgen.org/species/pinus-cembra/ accounting for 2 February 2020). The fronts of the major glaciers in the area are near the tree sampling area, since the Careser Glacier is ~3 km to the northeast, while the Venezia and La Mare glaciers are ~5 km to the west. In this area, individual Swiss stone pines are scattered in a treeline ecotone where ericaceous species are dominant (*Rhododendron ferrugineum* L., *Vaccinium* spp., Andreis and others, 2005; Gentili and others, 2013), growing on immature and thin podzols, histosols and umbrisols (Galvan and others, 2008). The trees are located in an area characterized by steep slopes, which prevent the possibility of thick snow accumulation. Moreover, the general south-oriented aspect of the area shields the trees from northerly winds, thus reducing the impact of frost desiccation (Oberhuber, 2004; Carturan and others, 2012; Cerrato and others, 2019).

We sampled 24 tree cores from the 12 dominant Swiss stone pines that were closest to the Careser Glacier (Fig. S2 in Supplementary Material), and these samples were processed according to standard techniques (Schweingruber and others, 1978; Schweingruber, 1988). The MXD data were obtained by means of an ITRAX multiscanner, following the protocol of Gunnarson and others (2011). The individual MXD series from each tree were standardized using data-adaptive age-dependent spline smoothing with 50 years of stiffness and a signal-free approach to obtain an MXD site chronology (Melvin and others, 2007). The detailed description of the tree-ring dataset is reported in Cerrato and others (2019).

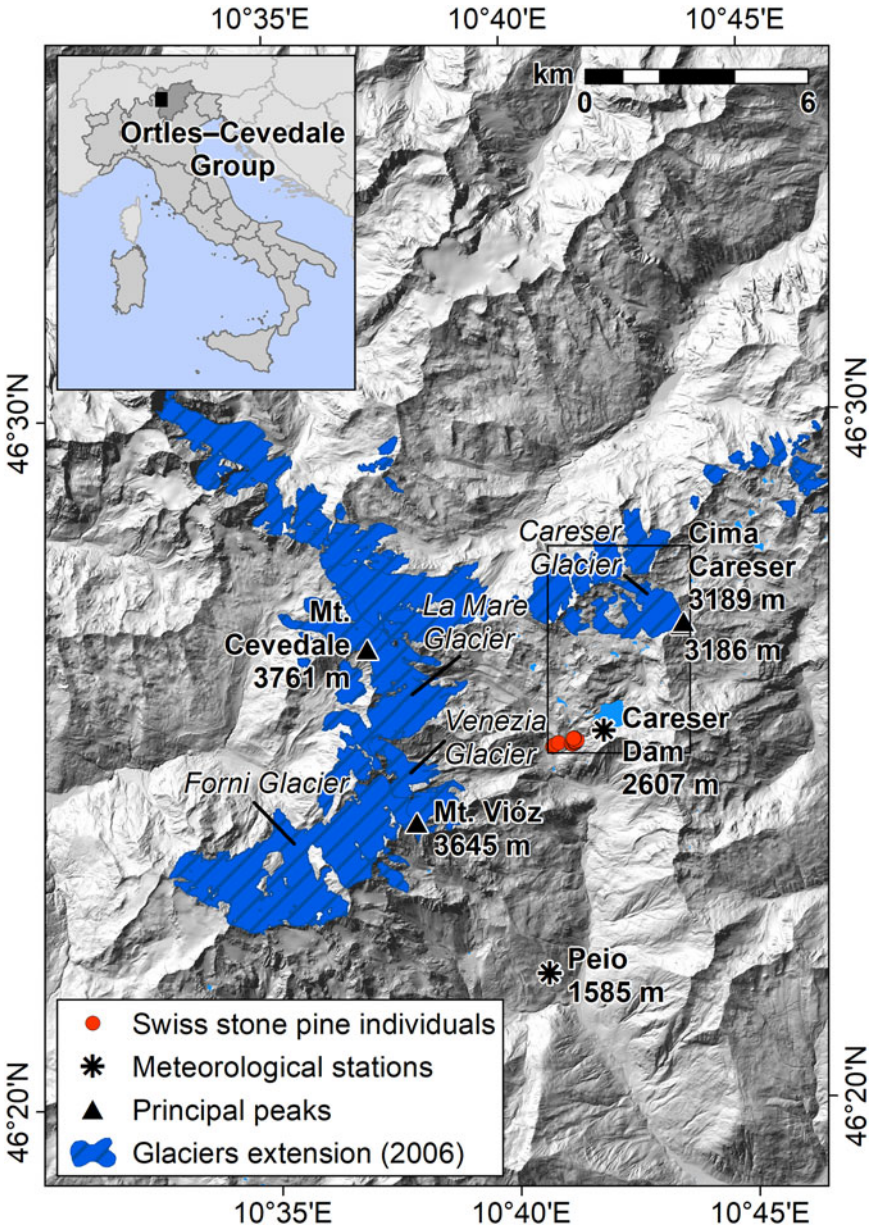

Fig. 1. Location map of the study area. For the colour image, please refer to the online version of this paper.

3.2 Glaciological and meteorological data

The annual mass balance (B_n) of the Careser Glacier has been continuously measured since 1967 (Zanon, 1992; Carturan and others, 2013a; Baroni and others, 2018) using the direct glaciological method (Østrem and Brugman, 1991). Measurements of the winter and summer balances (hereafter, B_w and B_s respectively) are performed separately, since the transition between the accumulation and ablation seasons is distinct. The latter season spans from May to September, as described in detail by Carturan and others (2013a). However, seven non-contiguous years (1979/80, 1980/81, 1985/86, 1986/87, 1998/99, 1999/2000, 2001/02) of seasonal mass-balance measurements are missing (Carturan and others, 2013a; Baroni and others, 2018). To estimate the missing data in the seasonal dataset, the B_s values were inferred from the B_n by means of a single linear regression, which was possible since the Careser Glacier B_s, as a single regressor, explains 89% of the B_n variance, while the relative importance of this variable in a multiple regression is 83%. The estimated B_w values were calculated as the difference between B_n and the inferred values of B_s. Estimating B_s (and B_w) from B_n was preferred to estimating these values from temperature, since B_n explains a higher fraction of the B_s variance compared to temperature (89 vs 74%, respectively).

Long-term monthly temperature (T) and precipitation (P) series were reconstructed for the Careser Glacier site by exploiting the long meteorological series available for the Alpine region over the periods of 1774–2017 and 1800–2017 for T and P, respectively (Brunetti and others, 2012, 2014; Crespi and others, 2018). The meteorological data were interpolated at the glacier site using the anomaly method (New and others, 2000; Mitchell and Jones, 2005), as described in Brunetti and others (2012, 2014) and Crespi and others (2018). For the present work, climatic data between 1811/12 and 2012/13 were considered for analysis with the overlapping tree-ring series.

3.3 Tree-ring, climatology and mass-balance correlations and reconstructions

Considering the glacier seasonal mass-balance series of the Central European region (thus including the Pyrenees and the Apennine glaciers) over the 1950–2010 period, the influence of B_w on B_n is limited, explaining 6% of the annual average

variance (Zemp and others, 2015). However, in the southern Rhaetian Alps, the B_w of the Careser Glacier explains ~17% of B_n variability, although most of the annual variance can be explained by B_s (83%) over the 1967–2010 period (Carturan and others, 2013a, 2013b). Thus, an annual mass-balance reconstruction of this particular glacier based on a summer temperature-sensitive proxy, such as TRW or MXD, would provide a biased result and, consequently, a B_n reconstruction based on independently reconstructed B_s and B_w values was preferred.

Since avalanche contributions and winter ablation can be considered negligible (Carturan and others, 2013a), the precipitation amount during the accumulation period (October to May) was used as a predictor of B_w (predictand) in the linear regression and scaling model. Scaling is a methodology used in dendroclimatology to reconstruct temperature variations (e.g. Esper and others, 2002), and it equalizes the mean and std dev. of a proxy to the values of a time series record over a defined period of overlap (Esper and others, 2005).

Two reconstructed B_s series were calculated using the interpolated temperature and the MXD data as predictors, respectively, and the measured B_s as predictand in simple linear regression and scaling models. The Swiss stone pine MXD data can be used to reconstruct B_s, by exploiting the strong correlation that both variables show with the mean temperature of the May to September period (MJJAS hereafter; Carturan and others, 2013a; Cerrato and others, 2019). A linear regression model between MXD data and B_s has been successfully applied to reconstruct the B_s of a Scandinavian glacier using Scots pine MXD (Linderholm and others, 2007). The reconstructed B_n series were obtained by adding the reconstructed scaled (or regressed) B_w and scaled (or regressed) B_s values for each mass-balance year, since the beginning of the MXD data series in 1811/12 to 1966/67, when glaciological measurements were started. The B_n obtained as the sum of the B_s reconstructed by the interpolated temperature and the B_w reconstructed using precipitation is identified as 'temp/prec-based B_n' hereafter; the B_n obtained as sum of the B_s reconstructed by MXD and B_w reconstructed using precipitation is identified as 'MXD/prec-based B_n'.

It has been argued that for both MXD and B_s, the relationships with temperature have changed very recently (Carturan and others, 2013a; Cerrato and others, 2019). Thus, an evolutionary split-sample approach was used to check the stability of B_s scaling and linear regression models, testing time windows from a length of 20 years (1967–1986) to a length of 46 years (1967–2012) with a 2-year step. The models were tested by using half of the window data to calibrate the coefficients, while the remaining data were used for validation. The quality of the correlations between MXD and temperatures, B_s and temperatures, and B_w and precipitation was evaluated using Pearson's correlation index (r), Spearman's correlation index (ρ), root mean squared error (RMSE) and mean absolute error (MAE). Furthermore, the difference in the calculated RMSE between the calibration and validation windows (calculated as δRMSE = RMSE[calibration] − RMSE [validation]) and the difference between the δRMSEs of each split-sample procedure (calculated as ΔRMSE = δRMSE[1st half as calibration] − δRMSE[2nd half as calibration]) were analysed to evaluate the differences in RMSE among the different windows considered for calibration (from Tables S1 to S6 in Supplementary Material). Before calculating the coefficients of the scaling (or regression) models, the correlations between predictors and predictands, and their stability, were tested for the entire 1967–2013 period, using a moving correlation analysis with a moving window of 22 years and a step of 1 year.

To test the influence of the high- and mid-frequency domains on the total correlation values between the reconstructed and the measured B_n, a Gaussian-filtered series was calculated (window length = 30 years, sigma = 5 years) and used as mid-frequency series. High-frequency variability was calculated as the residual between the annual values and the mid-frequency series for both the reconstructed and the measured B_n. Finally, to test the reliability of the reconstructed series, a comparison was performed with the temp/prec-based B_n reconstruction of the Careser Glacier and with two B_n series of other glaciers in the Alps, for which the data exceed those of the Careser Glacier measured B_n (i.e. the Claridenfirn and Silvretta Glaciers, Huss and others, 2015; WGMS, 2017). Our test was based on the knowledge that, in the Alps, B_n shows high consistency over large distances, although B_w variability shows remarkable regional differences (Huss and others, 2015). Comparisons were also performed between nine other glaciers of the area, for which measured B_n series exist in the overlapping 1966/67–2012/13 period (for details on the series used, see Tables S7, S8 in Supplementary Material).

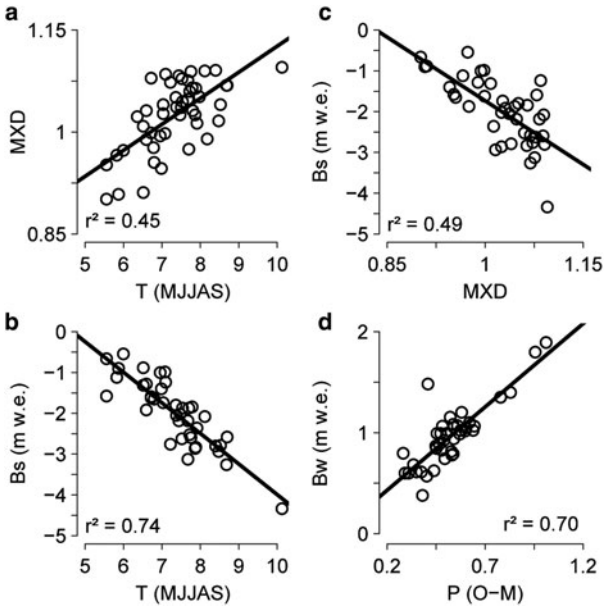

Fig. 2. The MXD data plotted against the mean May to September (MJJAS) temperature (a); the summer mass balance of the Careser Glacier plotted against the mean MJJAS temperature (b); the summer mass balance plotted against the MXD data (c); and the winter mass balance plotted against the winter precipitation (October to May) (d). All plots refer to the 1966/67–2012/13 period.

4. Results

4.1 Summer and winter mass balances

Considering the 1967–2012 period, the mean MJJAS temperatures have a strong influence both on B_s and on MXD, resulting in a significant p-value <0.01 and showing a higher correlation with the former ($r^2 = 0.74$) than with the latter ($r^2 = 0.45$). The correlation between B_s and MXD shows high and significant values (Figs 2a, b), indicating a relationship between the two variables ($r^2 = 0.49$; p-value <0.01; Table 1; Fig. 2c). However, the evolutionary split-sample procedures show an increasing difference in the obtained correlation values among B_s, MXD and temperature during the calibration period compared with those obtained during the validation period in both linear regression and scaling models. The differences become more important as soon as the more recent years are included in the considered window: more precisely, the years after 1992 when considering the MXD and B_s correlation (Figs S3, S6; Tables S1, S4 in Supplementary Material) and the years after 1996 when considering the B_s and temperature (Figs S4, S7; Tables S2, S5 in Supplementary Material) with both reconstruction models. A sudden increase

Table 1. Summary of the explained variance (r^2) between variables (May–September temperatures and October–May precipitations) and proxies (MXD, B_s and B_w)

	T_s (MJJAS)	B_s	P_w (O–M)	B_n
B_s	0.74*		0.01	0.89*
MXD	0.45*	0.49*	0.00	0.40*
B_w	0.01	0.03	0.70*	0.24†

Asterisks (*) and obelisks (†) identify values that are significant at a p-value <0.001 and 0.01, respectively.

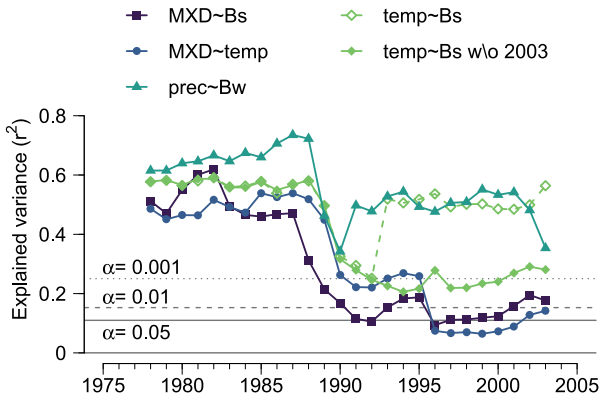

Fig. 3. Explained variance (22-year window, 1-year step, centred moving average) among the MXD, Careser Glacier summer mass balance and temperature and between the Careser Glacier winter mass balance and precipitation. For the colour image, please refer to the online version of this paper.

in the ΔRMSE since 2004 was clear (Figs S3, S4, S6 in Supplementary Material) in each reconstruction, with the exception of the scaling model between temperature and B_s (Fig. S7 in Supplementary Material). Increase in ΔRMSE is consistent with a decrease in the moving correlation values between MXD (or temperature) and B_s, calculated using a window-length of 22 years and a time-step of 1 year. We used a 22-year window because it represents the longest window that does not show large differences between the correlation values of the calibration and validation periods, as well as RMSE and MAE (Fig. 3; see Figs and Tables in Supplementary Material for details). In fact, a remarkable change in correlation values at ~1990 is noticeable (MXD~B_s, MXD~temperature and temperature~B_s), even if the values remain above the significance threshold of $\alpha = 0.05$ for most of the considered period (Fig. 3).

B_w is correlated with the winter precipitation from October of the previous year to May of the current year, with a mean explained variance of $r^2 = 0.70$ (p-value <0.01; Table 1; Fig. 2d). For the moving correlation and evolutionary split-sample procedure values, RMSE and MAE do not show significant differences in any considered windows during the 1967–2012 period (Fig. 3 and Figs S5, S8; Tables S3, S6 in Supplementary Material). The relationship between B_w and precipitation can be considered stable over the entire period considered (1966/67–2012/13, Fig. 3). Therefore, to be consistent with the B_s models, precipitation data from the 1966/67–87/88 period were used to build regression and scaling models of B_w back to 1811/12.

The statistical results of the selected 22-year window are reported in Table 2, together with the regression and scaling coefficients used. More details on other analysed windows are reported in the Supplementary Material (from Table S1 to S6).

4.2 Annual mass-balance reconstructions

A mass-balance estimate was calculated by applying both the regression and the scaling coefficients obtained using the 1966/67–87/88 calibration period of the two independent datasets (Table 2). In fact, the B_s and B_w values are independent, but were both significantly correlated with B_n (p-value <0.05). The reconstructed B_s, B_w and B_n showed good numerical and visual agreement with the measured balance series, capturing the long-term overall trend and the inter-annual variability, despite a tendency for the regression-based reconstructed balance to underestimate the measured B_n and B_s variance in comparison to the scaling-based reconstruction (Fig. 4).

The reconstructed B_n series based on MXD data reproduced the observed data with scaling and with the regression model quite well (Fig. 4). Both models reached a correlation value of $r = 0.73$ over the entire 1966/67–2012/13 period ($r^2 = 0.53$); instead, the correlation values between the measured and reconstructed B_n in the high- and mid-frequency domains were $r = 0.49$ ($r^2 = 0.24$) and $r = 0.89$ ($r^2 = 0.79$), respectively (Table 3). Considering only the calibration period characterized by the higher correlation values (1966/67–87/88), the correlation values increased to $r = 0.61$ ($r^2 = 0.37$) and $r = 0.92$ ($r^2 = 0.85$) for the high- and mid-frequency domains, respectively (the differences between scaling and regression were neglectable, see Tables S7, S8 in Supplementary Material). In comparison, the temp/prec-based B_n reconstruction over the whole period showed higher correlation values equal to $r = 0.87$ ($r^2 = 0.76$) with both scaling and regression models; instead, when considering high- and mid-frequencies separately, the correlation values were equal to $r = 0.80$ ($r^2 = 0.64$) and $r = 0.94$ ($r^2 = 0.88$). Considering only the calibration period, the obtained correlation values were $r = 0.84$ ($r^2 = 0.71$), $r = 0.83$ ($r^2 = 0.69$) and $r = 0.87$ ($r^2 = 0.74$) for the reconstructed series and the high- and mid-frequencies (Table 3).

The comparison between the reconstructed B_n of the Careser Glacier and the B_n of the Claridenfirn ($n = 52$) and Silvretta Glacier ($n = 48$) shows discrete agreement in both the high- and mid-frequency domains, considering both MXD/prec-based and temp/prec-based reconstructions with both scaling and regression models (Fig. 5; Table 3). Comparisons of the overlapping periods of measured B_n with other glaciers in the area are reported in Table 3 and in the Supplementary Material (Fig. S9).

The MXD/prec-based and temp/prec-based B_n reconstructions returned similar trends for most of the period, with the exception of the 1890–1920 window that alone accounted for ~58% of the total differences (Fig. 6), as also attested by the series highlighting the greatest differences in these decades. The series of differences show the absence of a statistically significant trend in the differences of the scaling model and a slightly significant trend for the regression model (Figs 6c, d). These outcomes are consistent with the 5-year running means of the reconstructed and measured B_n series that show good agreement until 1966/67, and with the measured B_n until 1994/95. After this year, the discrepancies become more important (Fig. 7).

The MXD/prec-based reconstructed B_n obtained by the scaling (regression) model shows 37 (24) years with positive values during the 1811/12–1965/66 period, and increases to 41 (26) including the period for which the measured series exists (1811/12–2012/13); meanwhile, temp/prec-based reconstructed B_n values show 50 (44) positive values during the 1811/12–1965/66 period, and increase to 55 (48) when also considering the 1966/67–2012/13 period. Of these positive values, 41% (42%) occurred during the 1811/12–49/50 period and 12% (8%) occurred during the 1960/61–79/80 period when considering the MXD/prec-based B_n reconstruction. Of the positive values reported by the temp/prec-based B_n reconstruction, 35% (38%) were highlighted during the 1811/12–49/50 period and 11% (10%) during the 1960/61–79/80 period.

Table 2. Summary of the calibration and verification statistics for the summer and winter mass-balance models

	Calibration			Validation statistics			1967–1988 period			
	Period	r^2	RMSE	Period	r^2	RMSE	r^2	RMSE	δRMSE	ΔRMSE
B_w_Scaling	1967–1977	0.87	120.95	1978–1988	0.36	276.21			155.26	
	1978–1988	0.36	244.77	1967–1977	0.87	128.86	0.62	197.19	−115.91	271.17
B_w_Regression	1967–1977	0.87	118.88	1978–1988	0.36	252.00			133.12	
	1978–1988	0.36	218.92	1967–1977	0.87	169.32	0.62	186.44	−49.60	−182.72
MXD_B_s_Scaling	1967–1977	0.30	403.02	1978–1988	0.42	273.61			273.61	
	1978–1988	0.42	332.60	1967–1977	0.30	369.92	0.50	384.39	369.92	−96.31
MXD_B_s_Regression	1967–1977	0.30	354.21	1978–1988	0.42	456.60			102.39	
	1978–1988	0.42	302.20	1967–1977	0.30	436.12	0.50	355.27	133.92	−31.53
Temp_B_s_Scaling	1967–1977	0.59	285.97	1978–1988	0.65	636.59			350.62	
	1978–1988	0.65	247.13	1967–1977	0.59	646.16	0.56	358.30	399.03	−48.41
Temp_B_s_Regression	1967–1977	0.59	269.09	1978–1988	0.65	491.46			222.37	
	1978–1988	0.65	234.93	1967–1977	0.59	534.03	0.56	334.85	299.10	−76.73

Scaling model equations:
B_w: $[(\Sigma P_{w(O-M)} - 539.965)/140.265] \cdot 309.879 + 998.397$ (1966/67–1987/88 calibration period)
MXD_B_s: $-[(MXD - 0.046)/0.990] \cdot 515.273 - 1468.306$ (1966/67–1987/88 calibration period)
Temp_B_s: $-[(\mu T_{s(M-S)} - 6.778)/0.702] \cdot 515.273 - 1468.306$ (1966/67–1987/88 calibration period)
Regression model equations:
B_w: $\Sigma P_{w(O-M)} \cdot 1.553 + 142.320$ (1966/67–1987/88 calibration period)
MXD_B_s: $-8001.660 \cdot MXD + 6452.347$ (1966/67–1987/88 calibration period)
Temp_B_s: $-548.061 \cdot \mu T_{s(M-S)} + 2246.551$ (1966/67–1987/88 calibration period)

More details on the indexes used can be found in Fritts (1976).
r^2, explained variance; RMSE, root mean squared error; δRMSE, difference between the RMSE values of the validation and calibration windows; ΔRMSE, difference between δRMSEs; B_w, winter balance; B_s, summer balance; $\Sigma P_{w(O-M}$, sum of the winter precipitation from October of the previous year to May of the current year; $\mu T_{s(M-S)}$, mean summer temperature from May to September.

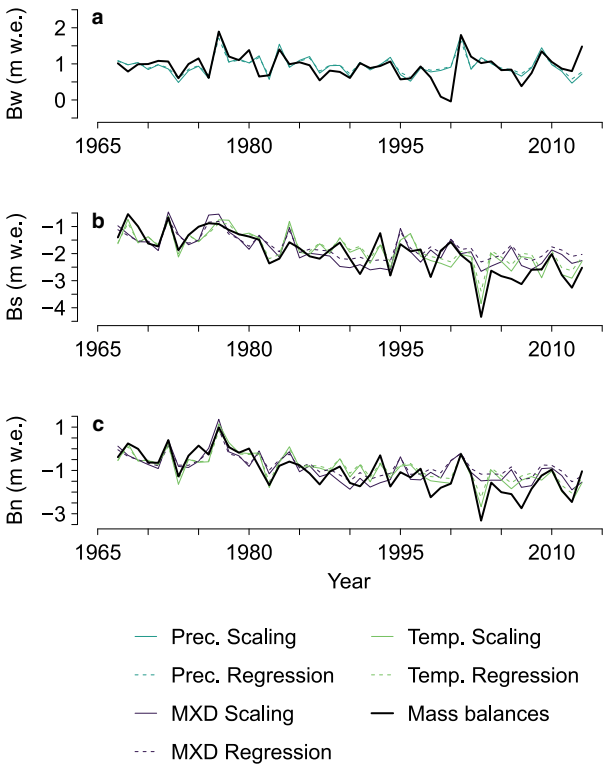

Fig. 4. Regression and scaling inferred mass balances from the MXD, temperature and precipitation and measured mass balances of the Careser Glacier (referred to the 1966/67–2012/13 period); B_w: winter (a); B_s: summer (b) and B_n: annual (c) mass balance. For the colour image, please refer to the online version of this paper.

On decadal timescales, the MXD/prec-based as well as the temp/prec-based reconstructed B_n show some periods with a slightly positive mass balance interrupting the general negative B_n trend. The periods with positive mass balances were: (i) from 1811/12 until the 1850s; (ii) in the ninth decade of the 19th century for the MXD/prec-based values, which extends to the 1910s, when considering the temp/prec-based B_n; (iii) during the second decade of the 20th century; and (iv) during the 1970s (1974/75–79/80). In contrast, periods with accentuated negative mass balances occurred: (i) in the 1904/05–10/11 period; (ii) during the second half of the 1940s; (iii) since 1986/87 (Fig. 7).

5. Discussion

On the basis of MXD-based and temperature-based reconstructions of B_s and the independently reconstructed B_w, Careser Glacier B_n estimates were calculated back to 1811/12. The higher correlation value between the B_s and B_n than between B_w and B_n for all the considered subperiods reported in Table 4 suggests that B_s was the main factor influencing the Careser Glacier annual mass balance before the start of glaciological measurements, at least on the long-term timescale. However, the significant correlation between B_w and B_n highlights the need for using independent proxies to reconstruct both seasonal balances (Table 4). The higher importance of B_w relative to B_n at the Careser Glacier is demonstrated by its higher correlation value ($r_{BwBn} = 0.49$, note that in Table 1 values are reported as r^2), compared to the importance of the seasonal mass-balance series of other Central European glaciers relative to their B_n values ($r_{BwBn} = 0.24$, Zemp and others, 2015). This can be ascribed to the particular climatic conditions and to the shape of the Careser Glacier that yield autumn to spring precipitation as a more important factor. The Careser Glacier's location at the southern margin of the 'inner dry Alpine zone' enables the glacier to benefit from the absence of an evident dry season, with large amounts of precipitation occurring during the accumulation period (Isotta and others, 2014; Crespi and others, 2018). Additionally, owing to the shape of the glacier, feeding by snow avalanches and reduced melting caused by topographic shading are largely negligible (Carturan and others, 2014). The absence of significant changes in precipitation during the accumulation season for the Careser Glacier region (Brunetti and others, 2006; Carturan and others, 2013b) confirms and enforces the idea that although winter precipitation is an important factor for annual mass balance, the mean MJJAS temperatures are the crucial factor determining positive and negative annual mass balances.

Table 3. Pearson's correlation values between the measured annual balance of Alpine glaciers and both the measured and reconstructed Careser Glacier B_n values over the 1966/67–2012/13 period

				High-frequency			Mid-frequency		
	Careser	MXD_B_n	Temp_B_n	Careser	MXD_B_n	Temp_B_n	Careser	MXD_B_n	Temp_B_n
Allalin	0.73	0.63	0.67	0.68	0.39	0.61	0.83	0.90	0.75
Claridenfirn	0.72	0.56	0.72	0.58	0.17 (0.35)	0.58 (0.65)	0.90	0.88 (0.69)	0.91 (0.76)
Gietro	0.61	0.33	0.59	0.58	0.06	0.47	0.81	0.76	0.88
Gries	0.84	0.69	0.81	0.68	0.39	0.69	0.97	0.91	0.92
Hintereis	0.91	0.76	0.88	0.87	0.49	0.87	0.95	0.93	0.91
Hohlaub	0.57	0.45	0.54	0.48	0.25	0.46	0.71	0.68	0.68
Kesselwand	0.84	0.62	0.77	0.83	0.34	0.76	0.91	0.91	0.83
Schwarzberg	0.72	0.52	0.67	0.56	0.26	0.54	0.85	0.75	0.81
Silvretta	0.79	0.57	0.78	0.74	0.20 (0.46)	0.73 (0.70)	0.89	0.91 (0.53)	0.90 (0.56)
Stubacher	0.74	0.51	0.71	0.70	0.23	0.60	0.92	0.91	0.91
Vernagt	0.84	0.65	0.81	0.76	0.23	0.71	0.94	0.93	0.91
Careser		0.73	0.87		0.49	0.80		0.89	0.94

The values in brackets refer to the 1914/15–65/66 period for the Claridenfirn ($n = 52$) and to the 1918/19–65/66 period for the Silvretta Glacier ($n = 48$). Neglectable differences in correlation values were obtained by the regression and scaling models; thus, the results were not discerned.

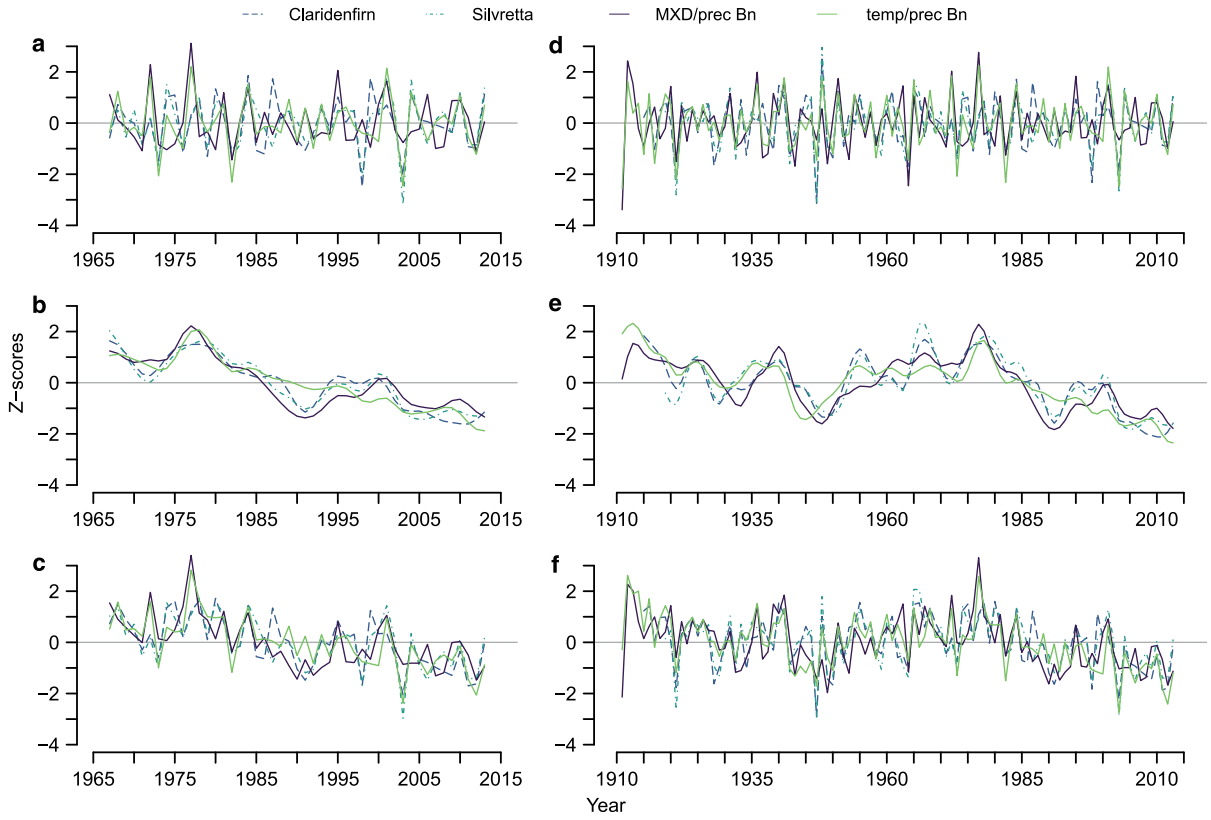

Fig. 5. *Z*-score values of the high-frequency domain (a and d), mid-frequency domain (b and e) and whole series (c and f) of reconstructed B_n values (MXD/prec-based B_s plus precipitation-based B_w, labelled as 'MXD/prec B_n', and temperature-based B_s plus precipitation-based B_w, labelled as 'temp/prec B_n') for the Careser Glacier obtained using the scaling models and *Z*-scores of the measured B_n of the Claridenfirn and Silvretta glaciers. The periods considered are 1966/67–2012/13 (left column) and 1910/11–2012/13 (right column). The *Z*-scores of the regression models are not reported because they were very similar to the *Z*-scores of the scaling models. For the colour image, please refer to the online version of this paper.

An overall good visual and statistical agreement is observed between the reconstructed and measured B_n during the calibration period (1966/67–88/89). However, a decrease in the modelling skill can be seen during the most recent period (1990/91–2012/13) in all the reconstructions (Figs 3, 4, 6, 7). When the modelling skills of the applied methods are compared, the scaling models better represent the measured B_n variations during the more recent period, whereas the regression models tend to return to a less-negative B_n (Fig. 6). These differences can be assumed marginal when considering: (i) the similarity of the RMSE between-models, which returned the values of 0.029 and 0.023 m w.e. for MXD-based and temperature-based reconstructions, and (ii) the similarity of the RMSE within-models, which account for 0.026 and 0.020 m w.e. of differences for scaling and regression models, respectively (Table 2).

As concerns the most recent period (from 1990s to date), the differences between the most negative B_s values recorded by the mass-balance measurements and the reconstructed B_s values are probably due to both: the decay of the Careser Glacier (Carturan and others, 2013a, 2016) and the loss of correlation between Swiss stone pine MXD and temperature (Cerrato and others, 2019), which denote non-linear behaviours of the two variables over the last three decades. Indeed, in the last 30 years, a dramatic and historically unprecedented period of

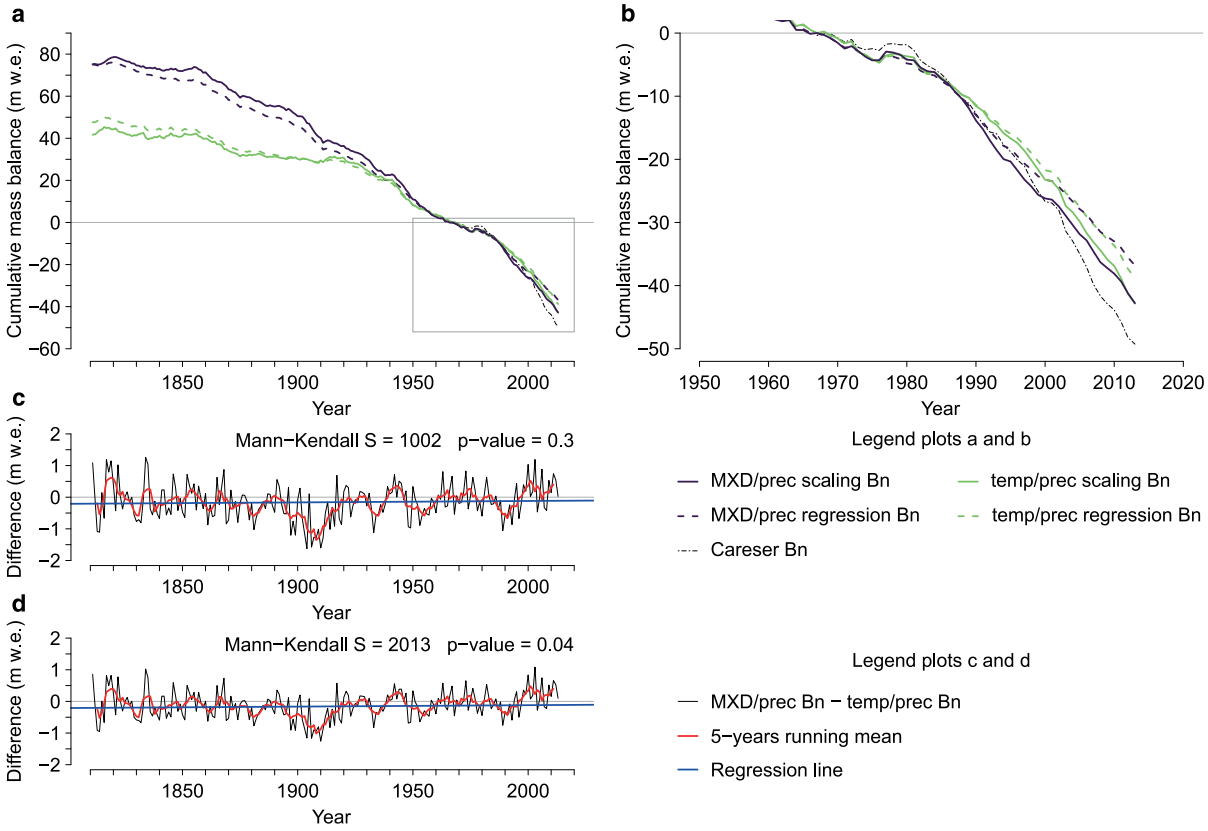

Fig. 6. Cumulative reconstruction of the Careser Glacier annual mass balance (B_n) for the 1811/12–2012/13 (a) and 1966/67–2012/13 periods (b). The arbitrary zero was set at the year 1966/67, when direct measurements began. Plot of the differences between the MXD/prec- and temp/prec-based B_n reconstructions using scaling (c) or regression (d) models. For the colour image, please refer to the online version of this paper.

negative-B_n years has occurred at the Careser Glacier (Carturan and others, 2013a; Baroni and others, 2017b, 2018), in the Ortles-Cevedale area (Carturan and others, 2013b), and at the regional and global scale (Salvatore and others, 2015; Zemp and others, 2015; Carturan and others, 2016). Because of its geometry (e.g. bedrock shape and hypsography), since the 1990s the Careser Glacier has been completely below its equilibrium line altitude (ELA), lacking an accumulation area and acting as a stagnant melting block of ice, as described by Carturan and others (2013b). ELA increase enhanced the ablation recorded at the Careser Glacier, which made the mass loss rates double the Ortles-Cevedale group mean rates (Carturan and others, 2013b), and a correlation decrease occurred between the glaciological measured B_s and temperature. The recorded melt rate is also a consequence of the thinning and fragmentation of ice masses, the enlargement of rocky windows and outcrops, and the lower albedo that during the last decades affected the Careser Glacier, caused by the ELA increase (Carturan and others, 2013a, 2016). Likewise, since the 1950s, the local Swiss stone pine MXD sensitivity to the mean MJJAS temperatures (in the high-frequency domain) has also gradually decreased and approached the critical correlation values during the same period in which the Careser Glacier began to show an accelerated melting rate, approximately in the 1990s (Figs 3, 4; Cerrato and others, 2019). This decrease is likely to have been induced by the rise in the mean summer temperatures (MJJAS) recorded at the sampling site (Carturan and others, 2013b), and also globally (IPCC, 2018) it could be related to the so-called 'divergence problem'. The loss of prediction capability by a tree species has been recorded aleatorily but ubiquitously at various latitudes and altitudes in the Northern Hemisphere, and among other causes, it is ascribed to the increasing temperature that recently may have created climatically optimal conditions for some high-altitude and high-latitude species (D'Arrigo and others, 2008) also in the studied area (Coppola and others, 2012; Leonelli and others, 2016). This 'divergence problem' implies that species that were stressed by summer low temperatures in the past are less stressed nowadays, lowering their capability to react to the temperatures. However, the 'divergence problem' might not be the only issue affecting the most recent end of MXD chronology; other factors such as common standardization or data collection methodology may influence MXD (Cook and others, 1995; Björklund and others, 2019). As a result of the accelerated melt rate of the Careser Glacier and of the loss of sensitivity of the Swiss stone pine MXD, which biases the proxies in opposite directions, the temp/prec-based reconstructed B_n series lies between the measured B_n and the MXD/prec-based B_n reconstruction but closer to the latter, supporting the concept that the change in Careser Glacier behaviour is the most important factor that has affected the B_n series in the last years (Fig. 7).

MXD/prec-based reconstruction well agrees with the temp/prec-based reconstruction, reporting a Pearson correlation value higher than 0.60 ($r^2 = 0.36$) over the 1811/12–1965/66 period when considering the total and filtered frequency domain (Table 4). The different models used for the reconstruction return similar results, with the B_n based on regression models showing a more contracted variance compared to the B_n based on scaling models (Fig. 4). This can be interpreted as an effect of the regression functions that reduce the amplitude of the reconstructed variable by the square root of the unexplained regression variance (Esper and others, 2005). Therefore, the reduction of the amplitude is more appreciable for MXD than for temperature and precipitation, since the unexplained variance of the MXD parameter is slightly higher than that of the temperature and precipitation

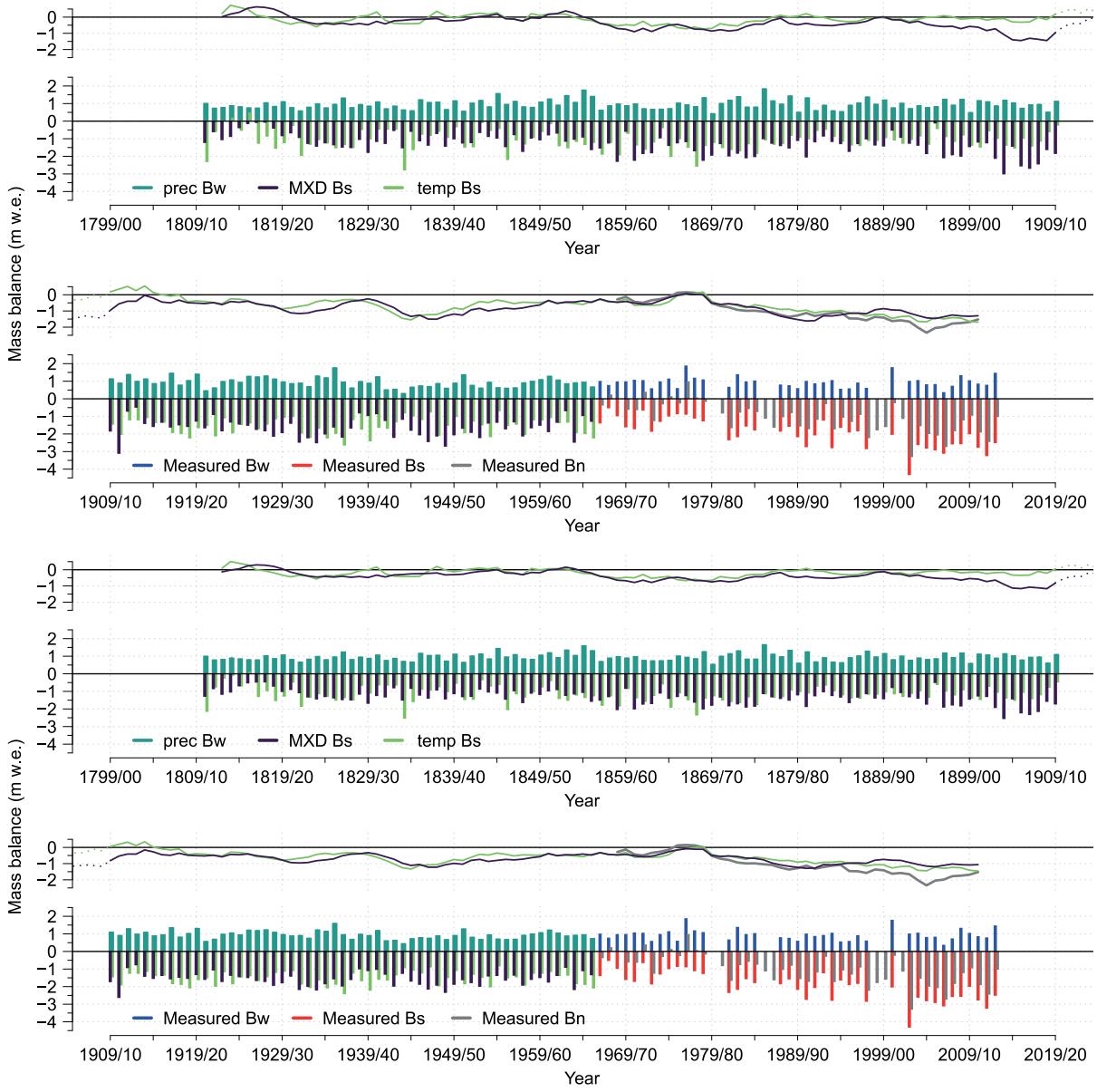

Fig. 7. The calculated Careser Glacier B_s and B_w mass balances for the 1810/11–1965/66 period and the measured record for the 1966/67–2012/13 period for scaling (upper panels) and regressing (lower panels), respectively. The lines represent the B_n 5-year running means. For the colour image, please refer to the online version of this paper.

Table 4. Correlation values (r^2) between mass-balance series (measured and reconstructed B_s, B_w and B_n obtained with the scaling model) over different periods

	1811/12–1965/66 period (n = 155)					1966/67–2012/13 period (n = 47)					1966/67–87/88 period (n = 22)					1988/89–2012/13 period (n = 25)				
	B_s*	B_s	B_w*	B_w	B_n*	B_s*	B_s	B_w*	B_w	B_n*	B_s*	B_s	B_w*	B_w	B_n*	B_s*	B_s	B_w*	B_w	B_n*
B_s*	*0.26*‡					*0.45*‡					*0.49*†					*0.05*				
B_s	–					0.48‡					0.50†					0.12				
						0.72‡					*0.66*‡					*0.54*‡				
B_w*	0.00	–				0.00	0.02				0.00	0.02				0.02	0.00			
	0.01					*0.01*					*0.03*					*0.04*				
B_w	–	–	–			0.00	0.01	0.46‡			0.02	0.07	0.62‡			0.07	0.03	0.36		
						0.03					*0.10*					0.01				
B_n*	0.82‡	–	0.19‡	–	0.37‡	0.81‡	0.44‡	0.25	0.13	0.74‡	0.74‡	0.44†	0.29	0.26	0.80‡	0.61‡	0.09	0.25	0.02	0.32
	0.24‡					*0.38*‡					*0.47*†					0.01				
	0.20‡		**0.24**‡			**0.38**‡	**0.65**‡	**0.22**	**0.18**		**0.33**	**0.50**†	**0.39**	**0.39**		**0.02**	**0.50**†	**0.10**	**0.04**	
	0.83‡					***0.84***‡					***0.78***‡					***0.76***‡				
B_n	–	–	–	–	–	0.40‡	0.83‡	0.16	0.25	0.53‡	0.37	0.80‡	0.22	0.44†	0.56‡	0.03	0.70‡	0.10	0.15	0.13
						0.65‡				**0.76**‡	*0.59*‡				**0.70**‡	*0.40*†				**0.60**‡

The asterisk (*) identifies reconstructed mass balances; the obelisk (†) identifies significant r^2 values at 95%; and the dagger (‡) identifies r^2 values significant at 99%. *Italic* values refer to temperature-based reconstructed B_s values. For B_n*: not-formatted values refer to MXD/prec-based reconstructed B_n values, whereas bold values refer to temp/prec-based reconstructed B_n values.

(Fig. 4). By contrast, the scaling model maintains a homogeneous variance between the predictor and the predictand, but it must be remembered that this model tends to inflate variance errors (Esper and others, 2005). Nevertheless, the differences between the diverse applied models are marginal for both MXD/prec-based and temp/prec-based reconstructions. In fact, the cumulative sum of the MXD/prec-based reconstructed B_n values for the 1811/12–1965/66 period suggests a total ice melt of 75 m w.e., considering both scaling and regression models. This value is lowered to 42 and 48 m w.e. when considering the temp/prec-based B_n reconstruction from the scaling and regression models, respectively. This difference of 30 ± 3 m w.e. is mainly due to the discrepancies highlighted during the first decade of the 20th century between the MXD/prec-based and temp/prec-based reconstructions, with the former reporting more negative values (Figs 6, 7). This difference might be caused by (or by a combination of) the MXD acquisition method (Björklund and others, 2019), by the standardization employed on the MXD data (Cook and others, 1995) or by the intrinsic diversity of the proxy and variable that were used to reconstruct the B_n. Even if the MXD is sensitive to the mean temperatures of the summer period from May to September (Cerrato and others, 2019), its value also depends on the growing season prone to length variations, and on the ablation season of the glaciers. Conversely, the mean monthly temperature has a fixed length; therefore, cold springs and/or autumns could positively affect the final B_s reconstructions (also reporting positive values occurring in the years 1812/13, 1813/14 and 1815/16 when considering scaling models and in 1815/16 when considering regression; Fig. 7). Moreover, the series of differences support the fact that the diversity between the B_n reconstructions is related to the characteristics of the dataset employed more than to a systematic bias like the one introduced during tree-ring series standardizations (Cook and others, 1995; Melvin, 2004). Indeed, if the loss of mid- and low-frequency (*sensu* Melvin, 2004) associated with MXD standardization had had a significant influence on the reconstruction, a significant trend in the differences should have been highlighted. On the contrary, in the investigated time period (1810/11–2012/13), the scaling reconstructions do not evidence any particular trend in the series of differences, which imply that MXD/prec- and temp/prec-based reconstructions retain the same trend. A slightly significant trend is highlighted in the series of differences related to the reconstructions obtained by the regression models, and is probably induced by the different angular coefficients used to reconstruct B_n (Fig. 6, Table 2).

The general negative trend that has occurred since the middle of the 19th century (Fig. 6), generally recognized as the end of the Little Ice Age in the Alps (LIA; Ivy-Ochs and others, 2009), is interrupted by the appreciably flattened or slightly positive mass balance in the MXD/prec-based B_n reconstruction and temp/prec-based B_n during the 1964/65–79/80 period and in the 1920s. Before the 1850/60s, the MXD/prec-based and temp/prec-based B_n reconstructions show another period of positive or slightly negative mass balances, with a first and higher maximum in the 1820s and a second in the 1850s (Figs 6, 7). These periods include ~70% of the reconstructed positive B_n based on MXD and on temperature with both models, and the highlighted periods perfectly match the historical evidence of stationarity or re-advances of the Italian glaciers (Baroni and Carton, 1990, 1996; Citterio and others, 2007; Carturan and others, 2013a; Salvatore and others, 2015; Baroni and others, 2016, 2017a, 2018) and of other European Alpine glaciers (Haeberli and others, 2007; Zemp and others, 2015). The calculated reconstructions of the B_n also highlight periods characterized by accelerated mass loss during the 1860s and the 1870s, between 1927/28 and 1934/35, in the 1940s and after the 1980s (Fig. 7). These findings comply with the observed Careser Glacier data series, which shows a long-term front retreat from 1933 to 1960 based on topographic data and geodetic differences and increasing mass loss rates after 1980 (Carturan and others, 2013a).

The topographic data make it possible to test the reliability of reconstructions by considering the 1932/33–1958/59 period, which is not included in the calibration/verification window. During this period, rates of −0.90 and −0.78 m w.e. a^{-1} characterized the calculated MXD/prec-based B_n obtained with the scaling and regression models, whereas values of −0.72 and −0.67 m w.e. a^{-1} were calculated for the temp/prec-based B_n. With regard to geodetic mass balances of the Careser Glacier, a rate of −0.70 m w.e. a^{-1} was calculated for the 1932/33–1958/59 period (Carturan and others, 2013a). These values are completely comparable, considering the systematic, random and spatial integration errors affecting the glaciological method (used in calibrations) and the systematic, random and density-correction errors affecting the geodetic method, all of which combine to result in the lowest detectable bias of ~0.3 m w.e. a^{-1} between the two methods (Zemp and others, 2013; Carturan, 2016). Before 1932/33, there are uncertainties affecting the calculation of geodetic ice loss rates, owing to the unknown period of the Careser Glacier LIA maximum and to approximations in the reconstruction of surface topography (Baroni and others, 2017b). Changes in the area-elevation distribution of the glacier that are negligible between 1932 and 1959 (ELA difference <10 m, Carturan and others, 2013a) further complicate comparisons prior to 1932/33, because at the LIA maximum, the ELA has been estimated to be 75 m lower than the one in 1932/33, thus affecting the mass balance of the glacier and probably requiring corrections before comparisons (Paul, 2010).

When the mid- and high-frequency trends of the reconstructed B_n are compared with the measured B_n values of other monitored glaciers in the Alps, each glacier appears to have its own driving processes, and therefore, generalization is difficult to accomplish in a climatically heterogeneous area like the Alps, but good correlation values are appreciable (Table 3). High correlation values in the mid-term frequency are appreciable between the proposed MXD/prec-based reconstruction and all the other B_n values considered, which in some cases are even higher than those among the measured B_n, especially during the 1987/88–2011/12 period (Table 3; Table S8 in Supplementary Material). These correlation values can be compared with those returned by the correlation with the temp/prec-based B_n reconstruction. This finding is consistent with the highlighted non-linear response of the Careser Glacier to the increasing temperature over the last 30 years and it supports the idea that the Swiss stone pine MXD can be used as a proxy for B_n reconstructions at least in the mid-frequency domain. In contrast, during the same period (1988/89–2012/13), the MXD/prec-based reconstructed B_n fails to coherently represent the high frequencies deriving from the influence of the divergence between the MXD data and temperature (Table 3; Table S7 in Supplementary Material). As a matter of fact, the temp/prec-based B_n reconstruction returns higher correlation values, with the other glacier B_n values in the high-frequency domain over the last decades. As concerns the period before 1966/67, the correlations show good values in both the high and mid frequencies, and the discrepancies relative to the B_n of the other glaciers can be ascribed to the different climatic conditions and dynamics characterizing the different ice bodies (Fig. 5).

6. Conclusions

The Swiss stone pine MXD data from the southern Rhaetian Alps are a promising tool for B_s reconstruction, since this proxy is sensitive to mean temperature during the whole ablation season

(May to September). The temperature signal is stable over time (Cerrato and others, 2019), unlike the other often-used tree-ring parameters (i.e. TRW, Leonelli and others, 2011). In particular, the MXD series results to be strongly, negatively correlated with the B_s.

The MXD data, coupled with the B_w independently inferred from precipitation observations, permitted a B_n variation estimate of the Careser Glacier back to the glaciological year 1811/12. Considering the agreement observed between the proposed B_n MXD/prec-based reconstruction and (i) temp/prec-based B_n reconstruction, (ii) glaciological data measured and (iii) past Careser Glacier extensions, we conclude that MXD data can be used as a proxy for the B_s of the Careser Glacier. Furthermore, on account of the similar trend shown by the proposed MXD/prec-based B_n reconstruction and by other Alpine glaciers, and considering the extended overlap between the natural range of the Swiss stone pine and the distribution of the glaciers in the European Alps, the Swiss stone pine, MXD data can be confidently applied as a proxy also to glaciers showing an ablation season moving alongside the Swiss stone pine growing season. Although there are quite a number of parameters other than temperature and precipitation (e.g. albedo, debris covering, glacier geometry and altitudinal distribution) affecting a glacier's mass balance, our results show the potential use of Swiss stone pine MXD data as a proxy for glaciological measurements with a higher degree of confidence than TRW. Even if winter precipitation can be considered an effective limit, new promising dendrochronological findings aimed at reconstructing this climatic variable in the Alpine region (Carrer and others, 2019) encourage further investigations on Swiss stone pine MXD as a proxy for B_s. Indeed, a great advantage of this proxy is that it can cover centuries with annual resolution and thus can improve and extend our glaciological knowledge further back in time.

Supplementary material. The supplementary material for this article can be found at https://doi.org/10.1017/jog.2020.40

Data availability. The dendrochronological data are freely accessible at the NOAA International Tree-Ring Data Bank (ITRDB) at the link: https://doi.org/10.25921/y4pb-3488.

Acknowledgments. This work was financially supported by the Italian MIUR Project (PRIN 2010–11): 'Response of morphoclimatic system dynamics to global changes and related geomorphological hazards' (national and local coordinator: C. Baroni) and by the project of strategic interest NEXTDATA (PNR National Research Programme 2011–2013; project coordinator A. Provenzale CNR-IGG, WP 1.6, leader C. Baroni UNIPI and CNR-IGG). We thank Göteborg University, Stockholm University, the University of Pisa and the Erasmus Programme Consortia Placement traineeship program for financial support. We are also grateful to Gino Delpero, Luca Colato and Mattia Delpero of Custodi Forestali – Comune di Vermiglio and Comune di Peio (TN) for helping with field activities and sampling. We thank Fabio Angeli, who is responsible for the Ufficio Distrettuale Forestale di Malè (TN). The English text has been edited by American Journal Experts (certificate verification key: C223-B25C-189B-3977-13EP). We are grateful to the editors and the anonymous reviewers for their valuable comments to this work.

Author contributions. This study was developed with contributions from all authors: RC carried out data analysis and laboratory work for the density data under the supervision of BEG and HWL. RC performed field sampling, with contributions from CB and MCS. RC, MCS, HWL, BEG, LC, MB and CB contributed equally to the interpretation, discussion and conclusions of this paper. LC provided an updated glaciological series. MB reconstructed the instrumental meteorological data. The text was written by RC and MCS, with contributions from CB, LC, MB, HWL and BEG. The project was directed, coordinated and funded by CB.

Conflict of interest. The authors declare that they have no conflicts of interest.

Disclaimer. Any use of trade, firm or product names is for descriptive purposes only and does not imply endorsement by the involved universities.

References

Anchukaitis KJ and 22 others (2017) Last millennium Northern Hemisphere summer temperatures from tree rings: Part II, spatially resolved reconstructions. *Quaternary Science Reviews* **163**, 1–22. doi: 10.1016/j.quascirev.2017.02.020.

Andreis C, Armiraglio S, Caccianiga M, Bortolas D and Broglia A (2005) *Pinus cembra* L. nel settore sud-Alpino Lombardo (Italia Settentrionale). *Natura Bresciana – Annuario del Museo Civico di Scienze Naturali di Brescia, Brescia* **34**, 19–39.

Auer I and 31 others (2007) HISTALP – historical instrumental climatological surface time series of the Greater Alpine Region. *International Journal of Climatology* **27**(1), 17–46. doi:10.1002/joc.1377.

Baroni C and 7 others (2017b) Double response of glaciers in the Upper Peio Valley (Rhaetian Alps, Italy) to the Younger Dryas climatic deterioration. *Boreas* **46**(4), 783–798. doi: 10.1111/bor.12284.

Baroni C, Bondesan A, Carturan L and Chiarle M (eds.) (2018) Report of the Glaciological Survey 2017. Relazioni della Campagna Glaciologica 2017. *Geografia Fisica e Dinamica Quaternaria* **41**(2), 115–193. doi: 10.4461/GFDQ.2018.41.17.

Baroni C, Bondesan A and Chiarle M (eds.) (2017a) Report of the Glaciological Survey 2016. Relazioni Della Campagna Glaciologica 2016. *Geografia Fisica e Dinamica Quaternaria* **40**(2), 233–320. doi: 10.4461/GFDQ.2017.40.14.

Baroni C, Bondesan A and Mortara G (eds.) (2016) Report of the Glaciological Survey 2015. Relazioni Della Campagna Glaciologica 2015. *Geografia Fisica e Dinamica Quaternaria* **39**(2), 215–295. doi: 10.4461/GFDQ.2016.39.20.

Baroni C and Carton A (1990) Variazioni oloceniche della Vedretta della Lobbia (Gruppo dell'Adamello, Alpi Centrali). *Geografia Fisica e Dinamica Quaternaria* **13**(2), 105–119.

Baroni C and Carton A (1996) Geomorfologia dell'Alta Val di Genova (Gruppo dell'Adamello, Alpi Centrali). *Geografia Fisica e Dinamica Quaternaria* **19**(1), 3–17.

Beniston M, Diaz HF and Bradley RS (1997) Climatic change at high elevation sites: an overview. *Climatic Change* **36**, 233–251. doi: 10.1023/A:1005380714349.

Björklund J and 41 others (2019) Scientific merits and analytical challenges of tree-ring densitometry. *Reviews of Geophysics* **57**(4), 1224–1264. doi: 10.1029/2019rg000642.

Böhm R and 5 others (2001) Regional temperature variability in the European Alps: 1760–1998 from homogenized instrumental time series. *International Journal of Climatology* **21**(14), 1779–1801. doi: 10.1002/joc.689.

Briffa KR, Osborn TJ and Schweingruber FH (2004) Large-scale temperature inferences from tree rings: a review. *Global and Planetary Change* **40**(1–2), 11–26. doi: 10.1016/S0921-8181(03)00095-X.

Brunetti M and 6 others (2009) Climate variability and change in the Greater Alpine Region over the last two centuries based on multi-variable analysis. *International Journal of Climatology* **29**(15), 2197–2225. doi: 10.1002/joc.1857.

Brunetti M and 5 others (2012) Projecting North Eastern Italy temperature and precipitation secular records onto a high-resolution grid. *Physics and Chemistry of the Earth, Parts A/B/C* **40–41**, 9–22. doi: 10.1016/j.pce.2009.12.005.

Brunetti M, Maugeri M, Monti F and Nanni T (2006) Temperature and precipitation variability in Italy in the last two centuries from homogenised instrumental time series. *International Journal of Climatology* **26**(3), 345–381. doi: 10.1002/joc.1251.

Brunetti M, Maugeri M, Nanni T, Simolo C and Spinoni J (2014) High-resolution temperature climatology for Italy: interpolation method intercomparison. *International Journal of Climatology* **34**(4), 1278–1296. doi: 10.1002/joc.3764.

Büntgen U and 10 others (2011) Causes and consequences of past and projected Scandinavian summer temperatures, 500–2100 AD. *PLoS ONE* **6**(9), e25133. doi: 10.1371/journal.pone.0025133.

Büntgen U, Esper J, Frank DC, Nicolussi K and Schmidhalter M (2005) A 1052-year tree-ring proxy for Alpine summer temperatures. *Climate Dynamics* **25**(2–3), 141–153. doi: 10.1007/s00382-005-0028-1.

Büntgen U, Frank DC, Nievergelt D and Esper J (2006) Summer temperature variations in the European Alps, A.D. 755–2004. *Journal of Climate* **19**(21), 5606–5623. doi: 10.1175/JCLI3917.1.

Carrer M, Pellizzari E, Prendin AL, Pividori M and Brunetti M (2019) Winter precipitation – not summer temperature – is still the main driver for Alpine shrub growth. *Science of the Total Environment* **682**, 171–179. doi: 10.1016/j.scitotenv.2019.05.152.

Carrer M and Urbinati C (2006) Long-term change in the sensitivity of tree-ring growth to climate forcing in *Larix decidua*. *New Phytologist* **170** (4), 861–872. doi: 10.1111/j.1469-8137.2006.01703.x.

Carturan L and 11 others (2013a) Decay of a long-term monitored glacier: Careser Glacier (Ortles-Cevedale, European Alps). *Cryosphere* **7**(6), 1819–1838. doi: 10.5194/tc-7-1819-2013.

Carturan L and 10 others (2013b) Area and volume loss of the glaciers in the Ortles-Cevedale group (Eastern Italian Alps): controls and imbalance of the remaining glaciers. *Cryosphere* **7**(5), 1339–1359. doi: 10.5194/tc-7-1339-2013.

Carturan L and 8 others (2014) Reconstructing fluctuations of La Mare glacier (Eastern Italian Alps) in the late Holocene: new evidence for a Little Ice Age maximum around 1600 AD. *Geografiska Annaler: Series A, Physical Geography* **96**(3), 287–306. doi: 10.1111/geoa.12048.

Carturan L and 7 others (2016) Analysis of the mass balance time series of glaciers in the Italian Alps. *Cryosphere* **10**(2), 695–712. doi: 10.5194/tc-10-695-2016.

Carturan L (2016) Replacing monitored glaciers undergoing extinction: a new measurement series on La Mare Glacier (Ortles-Cevedale, Italy). *Journal of Glaciology* **62**(236), 1093–1103. doi: 10.1017/jog.2016.107.

Carturan L, Dalla Fontana G and Borga M (2012) Estimation of winter precipitation in a high-altitude catchment of the Eastern Italian Alps: validation by means of glacier mass balance observations. *Geografia Fisica e Dinamica Quaternaria* **35**(1), 37–48. doi: 10.4461/GFDQ.2012.35.4.

Cerrato R and 7 others (2019) A *Pinus cembra* L. tree-ring record for late spring to late summer temperature in the Rhaetian Alps, Italy. *Dendrochronologia* **53**, 22–31. doi: 10.1016/j.dendro.2018.10.010.

Citterio M and 6 others (2007) The fluctuations of Italian glaciers during the last century: a contribution to knowledge about alpine glacier changes. *Geografiska Annaler: Series A, Physical Geography* **89**(3), 167–184. doi: 10.1111/j.1468-0459.2007.00316.x.

Cook ER, Briffa KR, Meko DM, Graybill DA and Funkhouser G (1995) The 'segment length curse' in long tree-ring chronology development for palaeoclimatic studies. *The Holocene* **5**(2), 229–237. doi: 10.1177/095968369500500211.

Coppola A, Leonelli G, Salvatore MC, Pelfini M and Baroni C (2012) Weakening climatic signal since mid-20th century in European larch tree-ring chronologies at different altitudes from the Adamello-Presanella Massif (Italian Alps). *Quaternary Research* **77**(3), 344–354. doi: 10.1016/j.yqres.2012.01.004.

Crespi A, Brunetti M, Lentini G and Maugeri M (2018) 1961-1990 high-resolution monthly precipitation climatologies for Italy. *International Journal of Climatology* **38**(2), 878–895. doi: 10.1002/joc.5217.

D'Arrigo R, Wilson RJS, Liepert B and Cherubini P (2008) On the 'divergence problem' in Northern Forests: a review of the tree-ring evidence and possible causes. *Global and Planetary Change* **60**(3–4), 289–305. doi: 10.1016/j.gloplacha.2007.03.004.

Esper J and 9 others (2018) Large-scale, millennial-length temperature reconstructions from tree-rings. *Dendrochronologia* **50**(August), 81–90. doi: 10.1016/j.dendro.2018.06.001.

Esper J, Cook ER and Schweingruber FH (2002) Low-frequency signals in long tree-ring chronologies for reconstructing past temperature variability. *Science (New York, NY)* **295**(5563), 2250–2253. doi: 10.1126/science.1066208.

Esper J, Frank DC, Wilson RJS and Briffa KR (2005) Effect of scaling and regression on reconstructed temperature amplitude for the past millennium. *Geophysical Research Letters* **32**(7), L07711. doi: 10.1029/2004GL021236.

Fritts HC (ed.) (1976) *Tree Rings and Climate*. Academic Press, London and New York.

Galvan P, Ponge J-F, Chersich S and Zanella A (2008) Humus components and soil biogenic structures in Norway spruce ecosystems. *Soil Science Society of America Journal* **72**(2), 548. doi: 10.2136/sssaj2006.0317.

Gentili R, Armiraglio S, Sgorbati S and Baroni C (2013) Geomorphological disturbance affects ecological driving forces and plant turnover along an altitudinal stress gradient on alpine slopes. *Plant Ecology* **214**(4), 571–586. doi: 10.1007/s11258-013-0190-1.

Gunnarson BE, Linderholm HW and Moberg A (2011) Improving a tree-ring reconstruction from west-central Scandinavia: 900 years of warm-season temperatures. *Climate Dynamics* **36**(1), 97–108. doi: 10.1007/s00382-010-0783-5.

Haeberli W, Hoelzle M, Paul F and Zemp M (2007) Integrated monitoring of mountain glaciers as key indicators of global climate change: the European Alps. *Annals of Glaciology* **46**, 150–160. doi: 10.3189/172756407782871512.

Huss M and 13 others (2017) Toward mountains without permanent snow and ice. *Earth's Future* **5**(5), 418–435. doi: 10.1002/2016EF000514.

Huss M, Dhulst L and Bauder A (2015) New long-term mass-balance series for the Swiss Alps. *Journal of Glaciology* **61**(227), 551–562. doi: 10.3189/2015jog15j015.

IPCC (2013) Summary for policymakers. In Stocker TF, Qin D, Plattner G-K, Tignor M, Allen SK, Boschung J, Nauels A, Xia Y, Bex V and Midgley PM (eds), *Climate Change 2013: The Physical Science Basis. Contribution of Working Group I to the Fifth Assessment Report of the Intergovernmental Panel on Climate Change*. Cambridge, UK and New York, NY, USA: Cambridge University Press, pp. 1–28.

IPCC (2018) Summary for policymakers. In Masson-Delmotte V, Zhai P, Pörtner HO, Roberts D, Skea J, Shukla PR, Pirani A, Moufouma-Okia W, Péan C, Pidcock R, Connors S, Matthews JBR, Chen Y, Zhou X, Gomis MI, Lonnoy E, Maycock T, Tignor M and Waterfield T (eds), *Global Warming of 1.5°C. An IPCC Special Report on the Impacts of Global Warming of 1.5°C Above pre-Industrial Levels and Related Global Greenhouse gas Emission Pathways, in the Context of Strengthening the Global Response to the Threat of Climate Change*. Geneva, Switzerland: World Meteorological Organization, p. 32.

IPCC (2019) *IPCC Special Report on the Ocean and Cryosphere in a Changing Climate*. [Pörtner, HO and 12 others (eds)]. In press. Available at https://www.ipcc.ch/report/srocc/.

Isotta FA and 17 others (2014) The climate of daily precipitation in the Alps: development and analysis of a high-resolution grid dataset from pan-Alpine rain-gauge data. *International Journal of Climatology* **34**(5), 1657–1675. doi: 10.1002/joc.3794.

Ivy-Ochs S and 5 others (2009) Latest Pleistocene and Holocene glacier variations in the European Alps. *Quaternary Science Reviews* **28**(21–22), 2137–2149. doi: 10.1016/j.quascirev.2009.03.009.

Kirdyanov AV, Vaganov EA and Hughes MK (2006) Separating the climatic signal from tree-ring width and maximum latewood density records. *Trees* **21**(1), 37–44. doi: 10.1007/s00468-006-0094-y.

Konter O, Büntgen U, Carrer M, Timonen M and Esper J (2016) Climate signal age effects in boreal tree-rings: lessons to be learned for paleoclimatic reconstructions. *Quaternary Science Reviews* **142**, 164–172. doi: 10.1016/j.quascirev.2016.04.020.

Larocque SJ and Smith DJ (2005) 'Little Ice Age' proxy glacier mass balance records reconstructed from tree rings in the Mt Waddington area, British Columbia Coast Mountains, Canada. *Holocene* **15**(5), 748–757. doi: 10.1191/0959683605hl848rp.

Leonelli G and 6 others (2016) Multispecies dendroclimatic reconstructions of summer temperature in the European Alps enhanced by trees highly sensitive to temperature. *Climatic Change* **137**(1–2), 275–291. doi: 10.1007/s10584-016-1658-5.

Leonelli G, Pelfini M and Cherubini P (2008) Exploring the potential of tree-ring chronologies from the Trafoi Valley (Central Italian Alps) to reconstruct glacier mass balance. *Boreas* **37**(1), 169–178. doi: 10.1111/j.1502-3885.2007.00010.x.

Leonelli G, Pelfini M, D'Arrigo R, Haeberli W and Cherubini P (2011) Non-stationary responses of tree-ring chronologies and glacier mass balance to climate in the European Alps. *Arctic, Antarctic, and Alpine Research* **43**(1), 56–65. doi: 10.1657/1938-4246-43.1.56.

Linderholm HW, Björklund J, Seftigen K, Gunnarson BE and Fuentes M (2015) Fennoscandia revisited: a spatially improved tree-ring reconstruction of summer temperatures for the last 900 years. *Climate Dynamics* **45**(3–4), 933–947. doi: 10.1007/s00382-014-2328-9.

Linderholm HW, Jansson P and Chen D (2007) A high-resolution reconstruction of Storglaciären mass balance back to 1780/81 using tree-ring data and circulation indices. *Quaternary Research* **67**(1), 12–20. doi: 10.1016/j.yqres.2006.08.005.

Ljungqvist FC and 8 others (2020) Assessing non-linearity in European temperature-sensitive tree-ring data. *Dendrochronologia* **59**(October 2019), 125652. doi: 10.1016/j.dendro.2019.125652.

Lowe JJ and 6 others (2008) Synchronisation of palaeoenvironmental events in the North Atlantic region during the Last Termination: a revised

protocol recommended by the INTIMATE group. *Quaternary Science Reviews* **27**(1–2), 6–17. doi: 10.1016/j.quascirev.2007.09.016.

Melvin TM (2004) *Historical Growth Rates and Changing Climatic Sensitivity of Boreal Conifers* (PhD dissertation). University of East Anglia, UK)

Melvin TM, Briffa KR, Nicolussi K and Grabner M (2007) Time-varying-response smoothing. *Dendrochronologia* **25**(1), 65–69. doi: 10.1016/j.dendro.2007.01.004.

Mitchell TD and Jones PD (2005) An improved method of constructing a database of monthly climate observations and associated high-resolution grids. *International Journal of Climatology* **25**(6), 693–712. doi: 10.1002/joc.1181.

New M, Hulme M and Jones PD (2000) Representing twentieth-century space–time climate variability. Part II: development of 1901–96 monthly grids of terrestrial surface climate. *Journal of Climate* **13**(13), 2217–2238. doi: 10.1175/1520-0442(2000)013<2217:RTCSTC>2.0.CO;2.

Nicolussi K (1995) Jahrringe und Massenbilanz. Dendroklimatologische Rekonstruktion der Massenbilanzreihe bis zum Jahr 1400 mittels *Pinus cembra*-Reihe.pdf. *Zeitschrift fur Gletscherkd. und Glazialgeol.* **30**, 11–52.

Oberhuber W (2004) Influence of climate on radial growth of *Pinus cembra* within the alpine timberline ecotone. *Tree Physiology*. **24**(3), 291–301. doi: 10.1093/treephys/24.3.291.

Oerlemans J (2001) *Glaciers and Climate Change*. Rotterdam: CRC Press, Tylor and Francis Group.

Østrem G and Brugman M (1991) *Glacier Mass-Balance Measurements: A Manual for Field and Office Work*. Saskatoon, Saskatchewan, Canada: National Hydrological Research Institute.

Paul F (2010) The influence of changes in glacier extent and surface elevation on modeled mass balance. *Cryosphere* **4**(4), 569–581. doi: 10.5194/tc-4-569-2010.

Peel MC, Finlayson BL and McMahon TA (2007) Updated world map of the Köppen-Geiger climate classification. *Hydrology and Earth System Sciences* **11**(5), 1633–1644. doi: 10.5194/hess-11-1633-2007.

Pepin N and 20 others (2015) Elevation-dependent warming in mountain regions of the world. *Nature Climate Change* **5**(5), 424–430. doi: 10.1038/nclimate2563.

Robertson I, Leavitt SW, Loader NJ and Buhay W (2008) Progress in isotope dendroclimatology. *Chemical Geology* **252**(1–2), EX1–EX4. doi: 10.1016/S0009-2541(08)00177-0.

Salvatore MC and 7 others (2015) The state of Italian glaciers: a snapshot of the 2006-2007 hydrological period. *Geografia Fisica e Dinamica Quaternaria* **38**(2), 175–198. doi: 10.4461/GFDQ.2015.38.16.

Schweingruber FH (1988) *Tree Rings Basic and Applications of Dendrochronology*. Dordrecht, The Netherlands: Springer. doi: 10.1007/978-94-009-1273-1.

Schweingruber FH, Fritts HC, Bräker OU, Drew LG and Schär E (1978) The x-ray technique as applied to dendroclimatology. *Tree-Ring Bulletin* **38**, 61–91. http://hdl.handle.net/10150/260420.

Watson E and Luckman BH (2004) Tree-ring-based mass-balance estimates for the past 300 years at Peyto Glacier, Alberta, Canada. *Quaternary Research* **62**(1), 9–18. doi: 10.1016/j.yqres.2004.04.007.

WGMS (2017) *Global Glacier Change Bulletin No. 2*. Zurich, Switzerland: ICSU(WDS)/IUGG(IACS)/UNEP/UNESCO/WMO, World Glacier Monitoring Service. doi: 10.5904/wgms-fog-2017-10.

WGMS and NSIDC (2012) *World Glacier Inventory*, Version 1. Boulder, CO, USA: NSIDC: National Snow and Ice Data Center. doi: 10.7265/N5/NSIDC-WGI-2012-02.

Wilson RJS and 22 others (2016) Last millennium northern hemisphere summer temperatures from tree rings: Part I: the long term context. *Quaternary Science Reviews* **134**, 1–18. doi: 10.1016/j.quascirev.2015.12.005.

Wood LJ and Smith DJ (2013) Climate and glacier mass balance trends from ad 1780 to present in the Columbia Mountains, British Columbia, Canada. *The Holocene* **23**(5), 739–748. doi: 10.1177/0959683612465450.

Wood LJ and Smith DJ (2015) Intra-annual dendroclimatic reconstruction for northern British Columbia, Canada, using wood properties. *Trees* **29**(2), 461–474. doi: 10.1007/s00468-014-1124-9.

Zanon G (1992) Twenty-five years of mass balance of the Careser Glacier, (Central Alps), 1966-67/1990-91. *Geografia Fisica e Dinamica Quaternaria* **15**, 215–219.

Zemp M and 16 others (2013) Reanalysing glacier mass balance measurement series. *Cryosphere* **7**(4), 1227–1245. doi: 10.5194/tc-7-1227-2013.

Zemp M and 38 others (2015) Historically unprecedented global glacier decline in the early 21st century. *Journal of Glaciology* **61**(228), 745–762. doi: 10.3189/2015JoG15J017.